BIOMICROFLUIDICS **8**, 052110 (2014)

An enzyme-linked immunosorbent assay on a centrifugal platform using magnetic beads

Chih-Hsin Shih,[1,a)] Ho-Chin Wu,[1] Chong-Yi Chang,[1] Wen-Hong Huang,[1] and Yi-Feng Yang[2]
[1]*Department of Chemical Engineering, Feng Chia University, 100 Wenhwa Road, Taichung 40724, Taiwan*
[2]*Shaoxing Pushkang Biotechnology Co., Ltd., 398 Mahuan Road, Binhai New Area, Shaoxing, Zhejiang Province 312366, People's Republic of China*

(Received 30 June 2014; accepted 11 September 2014; published online 19 September 2014)

An automated, disk-based, enzyme-linked immunosorbent assay (ELISA) system is presented in this work. Magnetic beads were used as the antibody carriers to improve the assay sensitivity and shorten the reaction time. The magnetic module integrated on the system is capable of controlling the magnetic beads to either move in the incubation stage or immobilize at a specific location during washing stage. This controlling mechanism utilizes a passive controlling approach so that it can be performed through disk spinning without the need of active control from external devices. The movement of the magnetic beads was investigated and the optimal rotational speed was found to be related to the ratio of the processing time to the cycle time of the magnetic beads. Comparing to ELISA conducted on microtiter plates, similar test results could be achieved by the disk-based ELISA but the entire protocol can be finished automatically within 45 min with much less reagent consumption. © *2014 AIP Publishing LLC*. [http://dx.doi.org/10.1063/1.4896297]

I. INTRODUCTION

Enzyme-linked immunosorbent assay (ELISA) is a widely used assay which quantifies chemical or biological molecules by utilizing the specificity between proteins, such as antibodies and antigens.[1] Conventionally, ELISA is carried out using microtiter plates. Its procedure includes several liquid adding and removing steps for reagents and wash buffers. A complete ELISA could take hours or even days. Many errors might occur during manual operations.[2] Therefore, it is desired to have ELISA carried out in a fast and automated way. In the last decade, it was proposed by many researchers to carry out ELISA on a disk platform (disk-based ELISA).[1–10] By utilizing the sequential flow control technique, reagents and wash buffers were delivered into the reaction chamber in sequence.[1,2,4,6,11] In addition, since the chemical reaction took place inside microchannel, the assay time was greatly reduced.[1,2,4,8,12,13] Therefore, a complete ELISA protocol can be performed on a disk platform through a programmed spinning control. Even though the disk-based ELISA has demonstrated its ability to be a better platform than the microtiter plate, there is still room for improvement. In most cases in the literature, the capture antibodies were immobilized on the surface of the reaction chamber. The mass transport between the antigens in the liquid and the antibodies on the solid surface is limited and so does the assay sensitivity.[1,2,4]

Magnetic beads emerged as an effective tool for bioassays.[12,14–16] For a fixed amount of sample volume, magnetic beads can greatly increase the surface-to-volume ratio of the reaction sites. In addition, the ability to control the mobility of the magnetic beads under magnetic field results in a better mass transport between the reactants. Therefore, the magnetic beads are

[a)]Author to whom correspondence should be addressed. Electronic mail: chshih@fcu.edu.tw. Tel.: +8864 24517250 ext 3680. FAX: +8864 24510890.

 © 2014 AIP Publishing LLC

superior to the solid surface as the antibody carrier. Assay sensitivity can be greatly improved through the application of magnetic beads.[14,17] Although magnetic beads were widely used in many microfluidic applications, handling magnetic beads was implemented mostly by manual operations.[12,18,19] Only a few approaches were reported with regard to the handling of the magnetic beads on the centrifugal platform. Cho *et al*. presented their work to control the location of the beads through a moving magnet, which was installed in a moving rail under the disk platform.[16] A primary magnet, which was mounted on a linear geared stepping motor installed underneath the moving rail, was used to control the position of the moving magnet. By coordinating the position of the primary magnet and the spinning directions, the moving magnet can be delivered to the desired locations. Strohmeier *et al*. presented their work to transport magnetic beads between three fluidically separated chambers through one stack of stationary permanent magnets and disk spinning control.[14]

In this work, we present a simple and effective mechanism to control the mobility of magnetic beads in both incubation and washing stages in the ELISA protocol. Our mechanism does not require any active control from external devices. All processes are encoded in the disk spinning program. Experimental results showed that using our system, a complete assay protocol can be conducted automatically within 45 min with assay results similar to the one conducted utilizing microtiter plates.

II. MICROFLUIDIC DESIGN AND THE MAGNETIC MODULE

The microfluidic design for the disk-based ELISA is shown in Fig. 1(a). It is composed of a substrate reservoir, a wash buffers reservoir, a mixing chamber, and a waste chamber. The spinning program for the disk-based ELISA is shown in Fig. 1(b). In the loading stage, wash buffer and substrate solution were loaded into each reservoir separately. Magnetic beads conjugated with capture antibodies, antigen solution, and detection antibodies labeled with horseradish peroxidase (HRP) were also loaded into the mixing chamber through the injection hole.

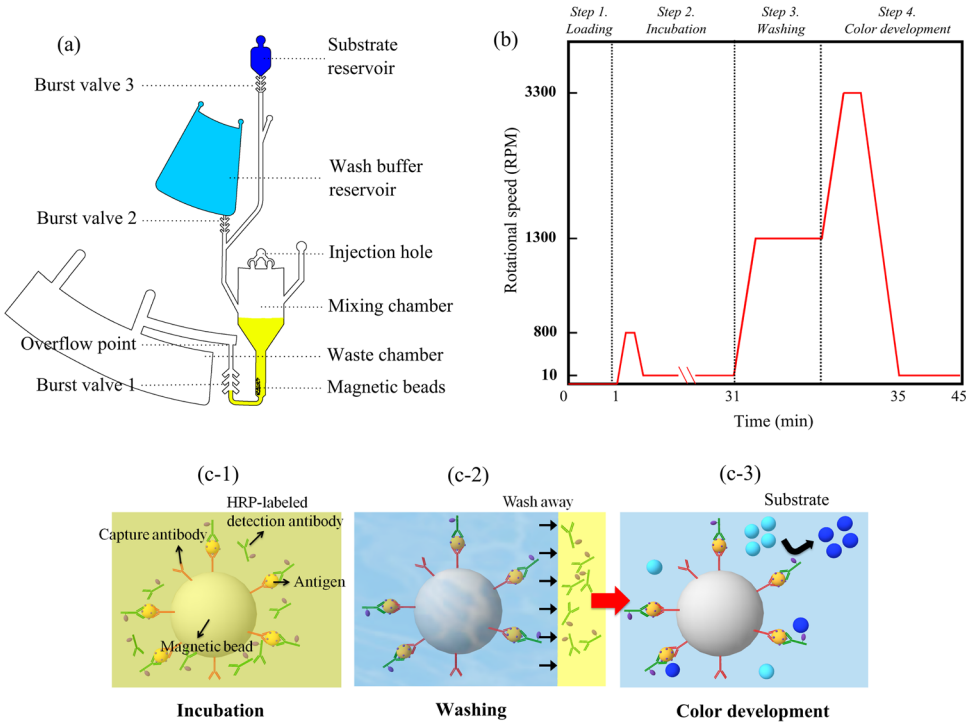

FIG. 1. (a) Schematic illustration of the microfluidic structure for the disk-based ELISA. (b) The operating procedures of the disk-based ELISA. (c) The reaction mechanism of disk-based ELISA in (c-1) the incubation stage, (c-2) the washing stage, and (c-3) color development.

Then, the disk was placed on the disk holder for processing. In the incubation stage, the disk started spinning from 0 to 800 RPM for 10 s to deliver the sample mixture into the mixing chamber, and then reduced to 10 RPM to incubate for 30 min. The burst valve between the mixing chamber and waste chamber (burst valve 1) stopped the liquid flow so that the liquid level was higher than the overflow point to the waste chamber. During this time, immunoreactions started so that antibodies and antigens formed a sandwich structure as shown in Fig. 1(c-1). In the washing stage, the rotational speed increased to 1300 RPM, and the wash buffer was released from the reservoir and flowed into the mixing chamber. The magnetic beads were immobilized by the moving permanent magnet and the unbounded materials were washed away into the waste chamber by the wash buffer solution (Fig. 1(c-2)). The liquid level in the mixing chamber was reduced to the same level as the overflow point. In the color development stage, the rotational speed was increased to 3300 RPM and the substrate solution was delivered into the mixing chamber. The substrate reacted with the HRP and developed color for signal detection (Fig. 1(c-3)).

The magnetic module used in this work is shown in Fig. 2. It is composed of three layers (Fig. 2(a)). The top layer is the magnet stage with eight stationary permanent magnets (NdFeB, N52, diameter = 5 mm, and height = 1 mm) distributed in a repeated pattern (**1** ($R_1 = 38$ mm), **2** ($R_2 = 32$ mm), **1** ($R_1 = 38$ mm), and **3** ($R_3 = 28$ mm)) between the inner and outer radial positions. The bottom layer is the disk holder with moving permanent magnets (NdFeB, N35, diameter = 2 mm, and height = 1 mm) inside magnet moving rails, whose structures are like trenches on the disk holder. The microfluidic disk is placed on the top of the disk holder but under the magnet stage. The stationary magnets and the moving magnets were aligned to be attractive.

The mechanism, which controls the motion of the magnetic beads in both incubation and washing stages, is described below. During the incubation stage, the disk was rotated at a low rotational speed ($\omega = 10$ RPM), the motions of the moving magnet and the magnetic beads were dominated by the magnetic attraction from the stationary magnet rather than centrifugal force. Our goal is to keep the moving magnet away from the mixing chamber so that it would not affect the motion of the magnetic beads during incubation. As shown in Fig. 2(b-2), when the mixing chamber passed by the stationary magnet **2**, the moving magnet was attracted by the stationary magnet **2** and moved to the middle of the moving rail. It was then dragged to the inner radial position of the moving rail by the stationary magnet **2** (Fig. 2(b-3)). When the mixing chamber passed by stationary magnet **1**, the distance between the moving magnet and the stationary magnet **1** is too far so that the moving magnet would not be attracted by the stationary magnet **1** and remained at the inner radial position of the moving rail (Fig. 2(b-4)). When the mixing chamber passed by the stationary magnet **3**, the moving magnet remained at the inner radial position of the moving rail by the attraction from the stationary magnet **3** (Fig. 2(b-6)). Therefore, the moving magnet was kept away from the mixing chamber during the incubation stage. On the other hand, the magnetic beads were attracted by the nearby stationary magnet when the mixing chamber approached the stationary magnet. As shown in Fig. 2(b), the magnetic beads traveled in a triangular route in the mixing chamber during the incubation stage. In comparison to immobilized antibodies on the chamber surface, the antibodies on the moving magnetic beads have better chance to capture the antigens in the mixing chamber so that the sensitivity can be improved and required incubation time can be reduced.

During the washing stage, the disk was rotated at a high rotational speed ($\omega = 1300$ RPM) in order to release the wash buffer stored in the inner radial position. Under this condition, the centrifugal force acted on the moving magnet was more dominant than the magnetic attraction from the stationary magnet. Therefore, the moving magnet moved to the outer radial position of the moving rail and remained at that position even when the mixing chamber passed by the stationary magnets during the entire washing process (Fig. 2(c)). The position of the moving magnet was designed to be at the left side of the exit of the mixing chamber since the effect of the Coriolis force would direct the magnetic beads to flow to the left side of the mixing chamber (under the counterclockwise disk rotation). Therefore, the magnetic beads would be captured by the moving magnet during the washing stage. Furthermore, in addition to the moving magnet, the chamber wall also provided supports needed to contain the magnetic beads. This is

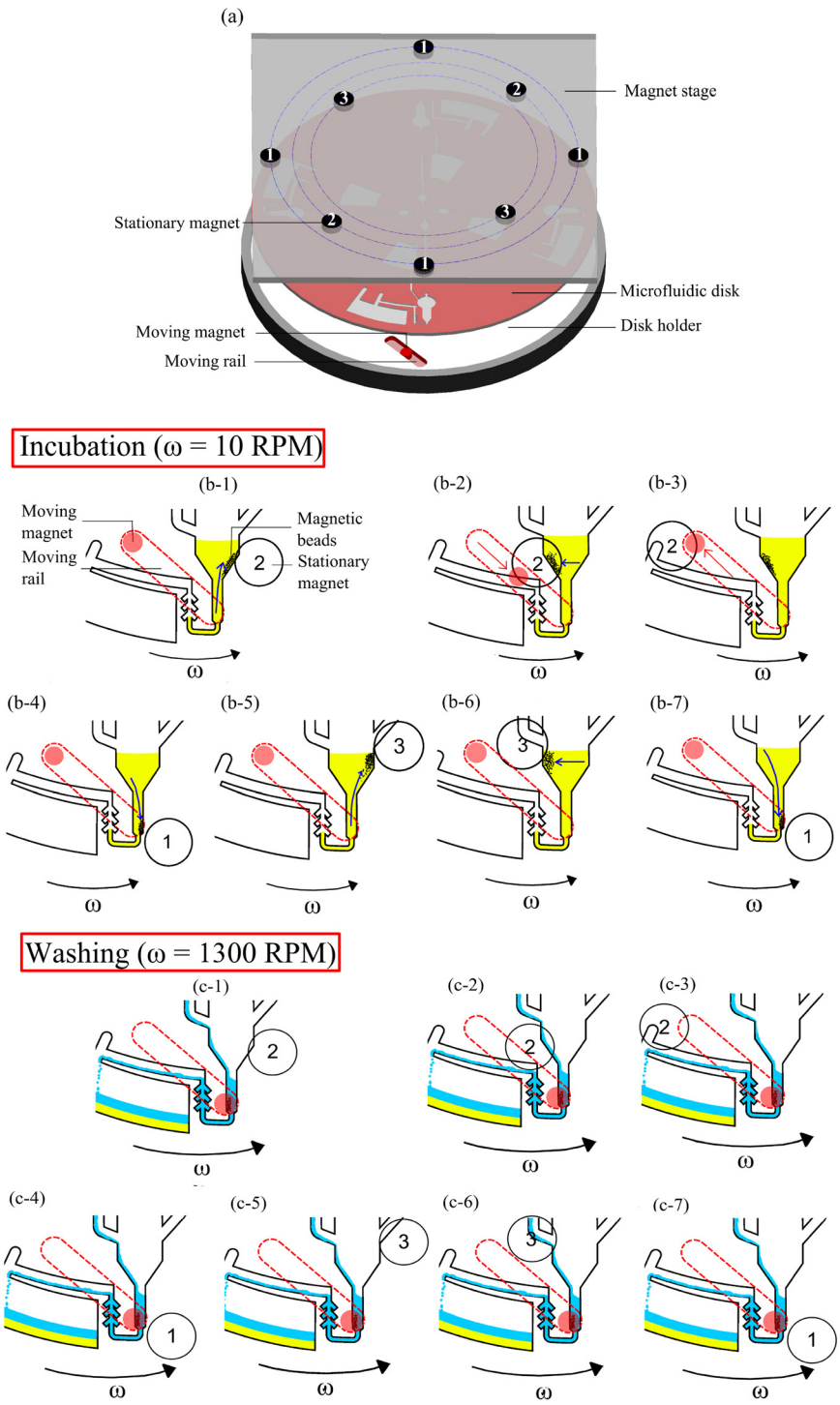

FIG. 2. Schematic illustration of the magnetic module and the controlling mechanism for the magnetic beads. (a) The magnetic module includes the magnet stage with 8 stationary permanent magnets, the microfluidic disk, and the disk holder with the moving permanent magnets inside the moving rails. (b) The movements of the magnetic beads and the moving magnet at the incubation stage ($\omega = 10$ RPM). The moving magnet was kept away from the mixing chamber while the magnetic beads moved towards the nearby stationary magnet. (c) In the washing stage ($\omega = 1300$ RPM), the moving magnet stayed at the outer radial position of the moving rail during the entire process. The magnetic beads were captured by the moving magnet and immobilized at the left side of the exit of the mixing chamber.

very important because our experimental results showed that part of the magnetic beads would be washed away if the moving magnet was located at the center of the exit of the mixing chamber rather than at the left side of the exit of the mixing chamber. This design ensures the magnetic beads to remain in the mixing chamber during the entire assay protocol. This controlling mechanism for the magnetic beads enables both incubation and washing to be carried out automatically. More consistent and repeatable ELISA test results can be obtained by utilizing this approach.

III. THEORY

A. Magnetic force

The magnetic force ($\vec{F}_m$) for a magnetic bead inside a magnetic field is described as

$$\vec{F}_m = \frac{v_p(\chi_p - \chi_m)}{\mu_0}(\nabla \cdot \vec{B})\vec{B}, \tag{1}$$

where χ_p and χ_m are the volumetric magnetic susceptibilities of the magnetic bead and the medium, respectively. v_p is the volume of the magnetic bead, $\vec{B}$ is the magnetic flux density that arises from the permanent magnet in the magnetic module, and μ_0 is the vacuum permeability constant (1.2566×10^{-6} N/A^2).

B. Viscous drag

The viscous drag force ($\vec{F}_{drug}$) on a magnetic bead can be defined as

$$\vec{F}_{drug} = 6\pi\eta R_0 \vec{V}_{term}, \tag{2}$$

where η is the viscosity of the medium, R_0 is the radius of the magnetic bead, and $\vec{V}_{term}$ is the terminal velocity of the magnetic bead. For a magnetic bead travel in a fluid under a magnetic field, the terminal velocity can be decided from the balance of the magnetic force and the viscous drag

$$\vec{V}_{term} = \frac{\vec{F}_m}{6\pi\eta R_0}. \tag{3}$$

C. Centrifugal and Coriolis force

During the spinning of the disk, centrifugation results in the centrifugal force ($\vec{F}_{cen}$) and the Coriolis force ($\vec{F}_{cor}$), which are described as

$$\vec{F}_{cen} = \rho\vec{\omega} \times (\vec{\omega} \times \vec{r}), \tag{4}$$

$$\vec{F}_{cor} = 2\rho(\vec{\omega} \times \vec{V}_{radial}), \tag{5}$$

where ρ is the density of the magnetic bead, $\vec{\omega}$ is the angular velocity of the disk-based platform, $\vec{r}$ is the distance of the magnetic bead from the center of the disk, and $\vec{V}_{radial}$ is the velocity of the magnetic bead in the radial direction.

IV. EXPERIMENTAL

A. Reagents

The magnetic beads (TANBeads® U-128) were purchased from Taiwan Advanced Nanotech Inc. (Taipei, Taiwan). They were modified with carboxyl group and have the diameter around 0.05 μm and the concentration of 200 mg/ml. Capture antibodies (mouse anti-human

IgG) purchased from BioCheck (Foster City, USA) were conjugated to the magnetic beads using covalent conjugation approach, and stored in a storage buffer (phosphate buffered saline (PBS) (-), 0.5% *bovine serum albumin* (BSA), 0.1% Tween 20, and 0.02% Proclin300, pH 7.4). Human chorionic gonadotropin (hCG) IgG purchased from BioCheck was stored in a fetal bovine serum (FBS) solution and used as the standards in this experiment. Anti-human IgG labeled with HRP purchased from BioCheck was used as the detection antibody. Tetramethylbenzidine (3,3′,5,5′-Tetramethylbenzidine, TMB) purchased from SurModics, Inc. (Eden Prairie, USA) was used as the substrate.

B. Disk fabrication

The microfluidic disk is composed of two layers. The bottom layer is a polymethylmethacrylate (PMMA) disk with the microstructures fabricated by an automatic engraving machine (EGX-350, Roland Corp.). The top layer is a clear polyolefin film coated with pressure-sensitive silicone-based adhesive purchased from 3M.

C. Microfluidic disk analyzer and flow visualization

The microfluidic analyzer consists of a spinning control system and signal detection system. The spinning control system includes a motor (HC-KFS13, Mitsubishi), which is managed by a computer program (LabVIEW, National Instruments) through a motor control card (PCI-7390, National Instruments). The detection system measures the optical signal from the disk and stores the information into the computer through a data acquisition card (PCI-6024e, National Instruments). The image-capturing system is composed of a complementary metal oxide semiconductor (CMOS) camera (SI-SV642C, EPIX), a stroboscope (DT-311N, SHIMPO), and a triggering sensor (PZ-V11, Keyence). The triggering sensor synchronizes the stroboscope with the spin frequency of the disk by detecting the reflected signals from the trigger mark on the disk. Computer software (Vision assistant, National Instruments) is utilized to analyze the experimental results from the images acquired by the CMOS camera.

V. RESULTS AND DISCUSSION

A. Process optimization for incubation

Effective reaction during incubation can greatly improve the assay sensitivity and reduce the time required for incubation. In order to find the optimal conditions to achieve high reaction conversion within a short period of time, a series of experiments were conducted by varying the concentration of the magnetic beads and the intensities of the magnetic field. To simulate the situation in ELISA, 1 μl of the HRP-labeled magnetic beads (1.042×10^{-3} mg/ml) were mixed with 99 μl of the magnetic-bead solutions (15, 30, and 90 mg/ml) to form the model solutions. 1 μl of the model solution was injected into the reaction chamber and incubated with 50 μl of the TMB substrate. The reaction rate was measured by the optical density of the substrate solution after incubating for 5 min. Higher optical density represented higher reaction rate.

The effect of disk rotational speeds on the reaction rate with various bead concentrations is shown in Fig. 3(a). In this experiment, the magnetic field strength measured from each permanent magnet is 225 mT. All curves showed similar trends. The optical density increased as the rotational speed increased (zone I) until reached a maximum value (zone II), then decreased afterwards as the rotational speed increased (zone III). The maximum reaction rate occurred at the rotational speed of 10 RPM for all concentrations of magnetic beads. Next, we conducted similar experiment by varying the magnetic field strength of the stationary permanent magnets (150 mT, 225 mT, and 350 mT) while utilizing the magnetic beads with the concentration of 15 mg/ml. As shown in Fig. 3(b), the optimal rotational speeds varied with the magnetic field strength. The optimal rotational speeds were 5, 10, and 20 RPM for the magnetic field strength of 150, 225, and 350 mT, respectively.

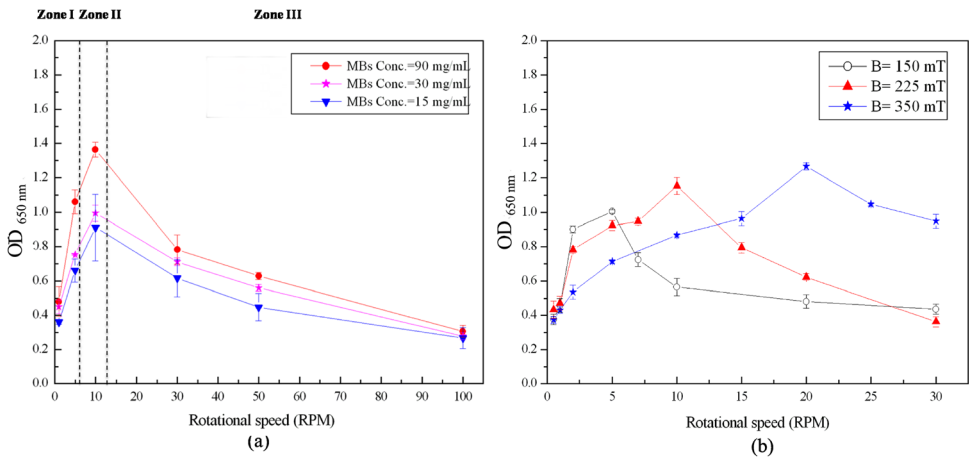

FIG. 3. The effect of disk rotational speeds on the reaction rate (represented by optical density) by varying (a) the concentration of the magnetic beads, and (b) the magnetic field strength of the stationary permanent magnets.

In order to further understand motion of the magnetic beads during incubation, flow visualization was conducted to observe the movement of the magnetic beads under various rotational speeds. The movements of the magnetic beads in three zones are summarized in Fig. 4. In zone

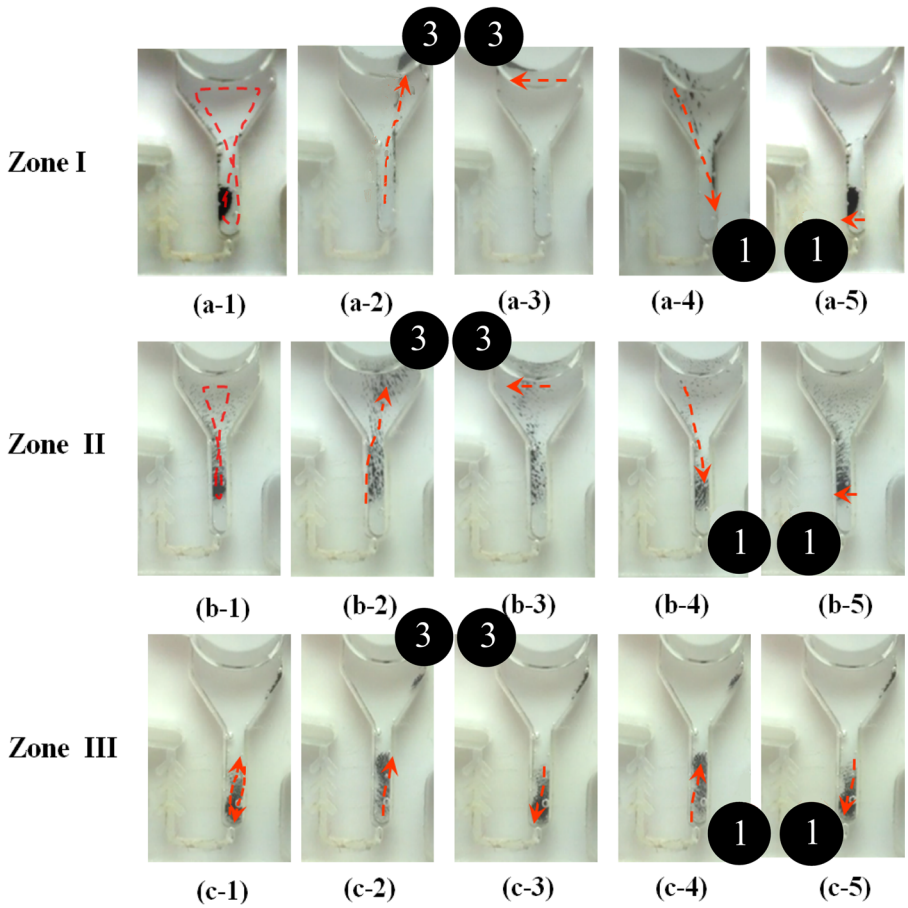

FIG. 4. The travel routes of magnetic beads at different rotational speeds. The numbered circles represent the stationary magnets. (a) In zone I ($\omega = 1$ RPM), the magnetic beads moved in a triangular route with idle time between each movement. (b) In zone II ($\omega = 10$ RPM), the magnetic beads moved dispersedly in a triangular path with very little idle time. (c) In zone III ($\omega = 30$ RPM), the movement of the magnetic beads was limited to a short range.

I, the disk was rotated at a very low rotational speed ($\omega = 1$ RPM) so that there was enough time for the magnetic beads to travel in a triangular route in the mixing chamber as shown in Fig. 4(a). In addition, there was idle time for the magnetic beads between each movement. Increasing the disk rotational speed increased the traveling distance of the magnetic beads so that the HRP-labeled magnetic beads tended to convert more substrate, which resulted in higher optical density. In zone II ($\omega = 10$ RPM), the magnetic beads still traveled in a triangular route but idle time between each movement was very little. In addition, as shown in Fig. 4(b), the magnetic beads moved dispersedly (comparing to the aggregate pack shown in Fig. 4(a)) so that the magnetic beads reacted with the substrate solution more effectively. The maximum optical density was observed in this zone. In zone III ($\omega = 30$ RPM), the high rotational speed resulted in shorter traveling range for the magnetic beads as shown in Fig. 4(c). The magnetic beads were only able to interact with limited amount of the substrate. The traveling range decreased as the rotational speed increased and so did the optical density of the solution.

From the above observation, we found that the optimal incubation condition is governed by two time constants: the cycle time (t_c) and the process time (t_p). For each revolution of rotation, the magnetic beads encountered N sets of stationary permanent magnets (N = 2 in this design, each set has 4 magnets), which provide the main driving force for the magnetic beads to move between the inner and outer radii in the mixing chamber. Therefore, the cycle time (t_c) for the magnetic beads during each set of the stationary permanent magnets is defined as

$$t_c = 60/w/N, \tag{6}$$

where ω is the rotational speed (RPM).

The process time (t_p) is defined as the time required for the magnetic beads to travel within certain distance under the magnetic field. The process time might vary with the magnetic field strength, the characteristics of the magnetic beads, and the liquid properties. In this study, the process time was measured through flow visualization. The process time is defined as the time required for the magnetic beads to travel in a distance of 4.5 mm in the radial direction. The process times measured in this experiment for various magnetic field strength are 0.43 s

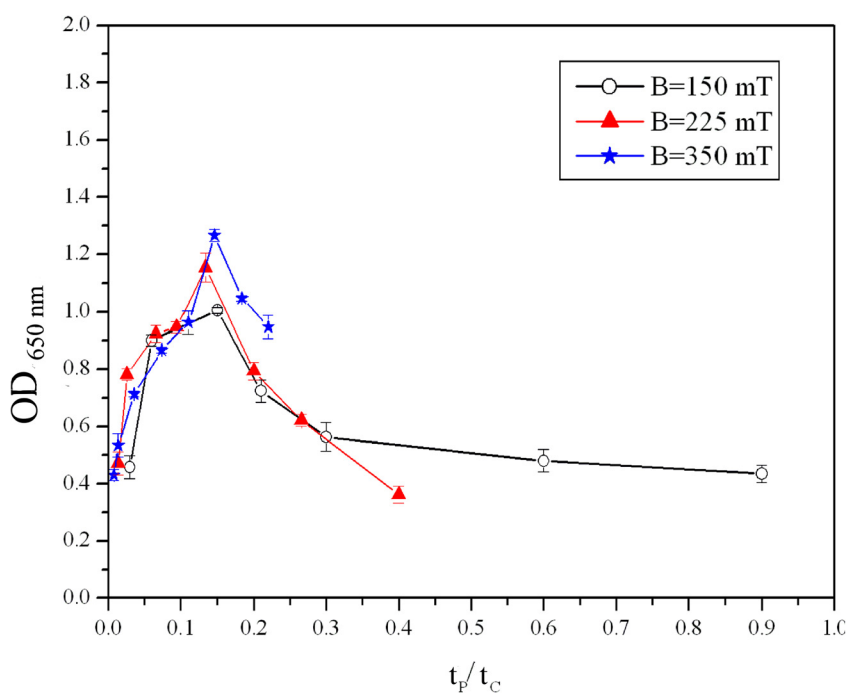

FIG. 5. The effect of the time ratio (the process time to cycle time) on the reaction rate (represented by optical density) under various magnetic field strength (150, 225, and 350 mT).

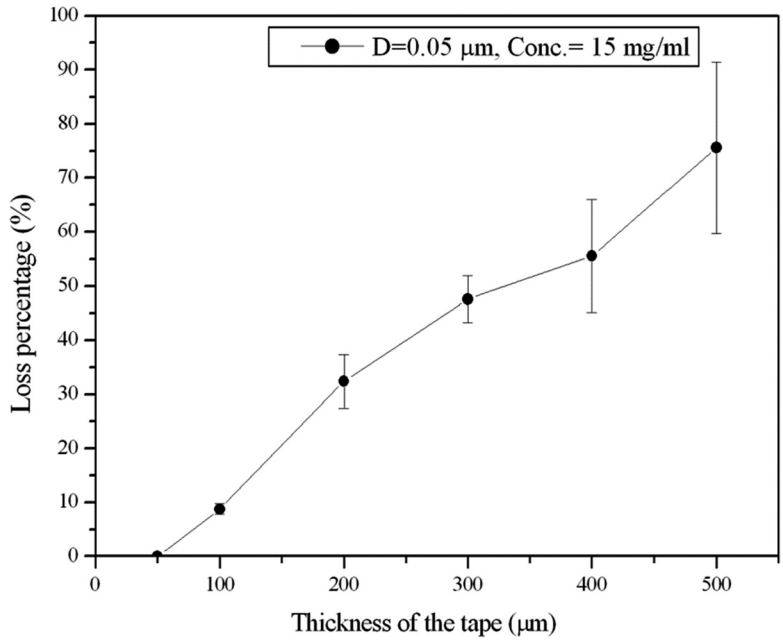

FIG. 6. The effect of tape thickness on the loss percentage of the magnetic beads under the rotational speed of 4000 RPM.

(150 mT), 0.27 s (225 mT), and 0.17 s (350 mT), respectively. By changing the x-axis in Fig. 3(b) from the rotational speed to the ratio of the process time to cycle time, the three distinct curves in Fig. 3(b) converged into a master curve. As shown in Fig. 5, the optimal reaction occurs when the time ratio is around 1.5 under various magnetic fields. This analysis can be used as a valuable tool to estimate the optimal rotational speed for the reaction induced by magnetic beads on a centrifugal platform.

B. Process optimization for washing

The major function for the moving magnet is to immobilize of the magnetic beads during washing ($\omega = 1300$ RPM) and substrate addition ($\omega = 3300$ RPM) steps. The thickness of the polyolefin tape, which is used to seal the microfluidic structure on the disk, plays an important role since it has a strong effect on the magnetic attraction of the moving magnet to the magnetic beads. Experiments were conducted to examine the effect of the tape thickness on the loss

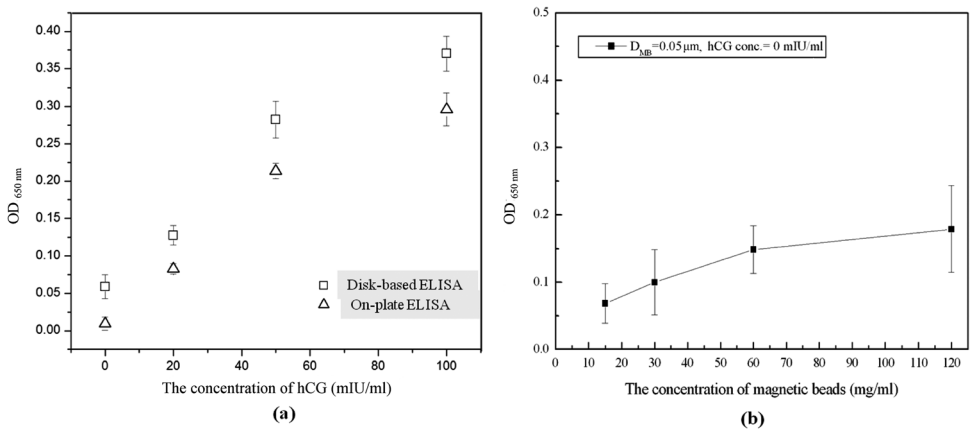

FIG. 7. (a) The comparison of the test results between disk-based ELISA and on-plate ELISA using magnetic beads. (b) The assay background signal for various concentrations of the magnetic beads after 10 min of incubation. The background signal increases as the concentration of magnetic beads increases.

TABLE I. Comparison of reagent volume and process time between on-plate ELISA and disk-based ELISA.

	Volume of reagent (μl)		Process time (min)	
Protocol	On-plate ELISA	Disk-based ELISA	On-plate ELISA	Disk-based ELISA
Antigen	50	50	30	30
HRP	100	1	30	
Washing	500 (5 times)	140 (1 time)	40 (two wash steps)	1
TMB	100	10	20	10

percentage of the magnetic beads under the rotational speed of 4000 RPM. As shown in Fig. 6, the loss percentage of the magnetic beads increases as the tape thickness increases. For the moving magnets used in this system, the tape thickness needs to be less than 50 μm in order to avoid the loss of the magnetic beads.

C. Disk-based ELISA

The disk-based ELISA was utilized to perform hCG detection and the test results were compared with the assays conducted using magnetic beads in the microtiter plate. As shown in Fig. 7(a), similar trend was observed between the disked-based ELISA and the one conducted using microtiter plates. In general, the signal from the disked-based is higher than the on-plate ELISA; this is due to the background induced by the magnetic beads. The iron oxide (Fe_3O_4) in the magnetic beads also reacts with TMB substrate for color development.[20] As shown in Fig. 7(b), the background signal increased as the concentration of the magnetic beads increased. Although the same effect also occurred in microtiter plates, the volume of TMB used in microtiter plates was ten times higher than the disk-based ELISA so that the background signal was diluted in microtiter plates. The comparison of the reagent consumption and the processing time between the disk-based ELISA and on-plate ELISA is shown in Table I. The disk-based ELISA consumes fewer reagents than the on-plate ELISA and the process can be finished in a shorter time (45 min vs. 2–3 h).

In comparison of our technologies to the previous work (CD ELISA without using magnetic beads) developed in the literature,[2] the previous work showed its superiority over the microtiter plate by having a larger specific surface area, which provides more area for the reaction sites, and shortening the diffusion length, which results in a faster chemical reaction. In our technology, for the same sample volume, the specific surface area can be easily enlarged by increasing the amount of magnetic beads, which have large specific surface area due to their small size (diameter around 50 nm). In addition, since the magnetic beads can be manipulated to move inside the mixing chamber, the reaction time required can be further reduced by changing the mass transport from diffusion to convection. Furthermore, in the previous work, surface chemistry needs to be developed in order to immobilize the antibody on the chamber surface, which varies according to the material used to fabricate the disk. Our approach is independent of the material used to fabricate the disk. Last, but not the least, in the previous work, the antibodies only reacted with the antigen in the reaction chamber. In our design, the magnetic beads conjugated with the capture antibodies can react with a larger sample volume (50 μl, as shown in Fig. 2(b)), and then collected in a smaller chamber (20 μl, as shown in Fig. 2(c)) for color development. The assay sensitivities can be further improved by this approach.

VI. CONCLUSIONS

In this study, an automated ELISA on a centrifugal platform was developed. A novel approach is proposed to manipulate the magnetic beads to promote mixing in the incubation stage and to immobilize in the washing stage. This passive approach is done by the coordination of the magnetic module and the disk spinning program without external active control

devices. Furthermore, the optimal rotational speed in the incubation stage could be estimated through the cycle time and process time analysis. We believe this analysis is an important tool for the mixing of magnetic beads on the centrifugal platform. Finally, the disk-based ELISA showed similar test results to the one conducted using microtiter plates. However, the disk-based ELISA can be performed automatically with less assay time and reagent consumption. It demonstrates great potential to be converted into a commercial product.

ACKNOWLEDGMENTS

This work was supported by Ministry of Science and Technology, Taiwan under Grant No. NSC 100-2221-E-035-071.

[1]H. He, Y. Yuan, W. Wang, N.-R. Chiou, A. J. Epstein, and L. J. Lee, Biomicrofluidics **3**, 022401 (2009).
[2]S. Lai, S. Wang, J. Luo, L. J. Lee, S. T. Yang, and M. J. Madou, Anal. Chem. **76**(7), 1832–1837 (2004).
[3]T.-H. Kim, K. Abi-Samra, V. Sunkara, D.-K. Park, M. Amasia, N. Kim, J. Kim, H. Kim, M. Madou, and Y.-K. Cho, Lab Chip **13**(18), 3747–3754 (2013).
[4]Y. Ukita, S. Kondo, T. Azeta, M. Ishizawa, C. Kataoka, M. Takeo, and Y. Utsumi, Sens. Actuators, B **166–167**, 898–906 (2012).
[5]U. Y. Schaff and G. J. Sommer, Clin. Chem. **57**(5), 753–761 (2011).
[6]B. S. Lee, Y. U. Lee, H. S. Kim, T. H. Kim, J. Park, J. G. Lee, J. Kim, H. Kim, W. G. Lee, and Y. K. Cho, Lab Chip **11**(1), 70–78 (2011).
[7]S. I. En Lin, Microfluid. Nanofluid. **9**(2–3), 523–532 (2010).
[8]B. S. Lee, J. N. Lee, J. M. Park, J. G. Lee, S. Kim, Y. K. Cho, and C. Ko, Lab Chip **9**(11), 1548–1555 (2009).
[9]H. Nagai, Y. Narita, M. Ohtaki, K. Saito, and S. I. Wakida, Anal. Sci. **23**(8), 975–979 (2007).
[10]N. Honda, U. Lindberg, P. Andersson, S. Hoffmann, and H. Takei, Clin. Chem. **51**(10), 1955–1961 (2005).
[11]J. Siegrist, R. Gorkin, L. Clime, E. Roy, R. Peytavi, H. Kido, M. Bergeron, T. Veres, and M. Madou, Microfluid. Nanofluid. **9**(1), 55–63 (2010).
[12]S. Qu, J. Liu, J. Luo, Y. Huang, W. Shi, B. Wang, and X. Cai, Anal. Chim. Acta **766**(0), 94–99 (2013).
[13]P. Andersson, G. Jesson, G. Kylberg, G. Ekstrand, and G. Thorsen, Anal. Chem. **79**(11), 4022–4030 (2007).
[14]O. Strohmeier, A. Emperle, G. Roth, D. Mark, R. Zengerle, and F. von Stetten, Lab Chip **13**(1), 146–155 (2013).
[15]N. Pamme, Lab Chip **6**(1), 24–38 (2006).
[16]Y. K. Cho, J. G. Lee, J. M. Park, B. S. Lee, Y. Lee, and C. Ko, Lab Chip **7**(5), 565–573 (2007).
[17]M. Grumann, A. Geipel, L. Riegger, R. Zengerle, and J. Ducree, Lab Chip **5**(5), 560–565 (2005).
[18]B. Esteban-Fernández de Ávila, V. Escamilla-Gómez, S. Campuzano, M. Pedrero, J. P. Salvador, M. P. Marco, and J. M. Pingarrón, Sens. Actuators, B **188**(0), 212–220 (2013).
[19]Z. Gao, M. Xu, L. Hou, G. Chen, and D. Tang, Anal. Chem. **85**(14), 6945–6952 (2013).
[20]L. Gao, J. Zhuang, L. Nie, J. Zhang, Y. Zhang, N. Gu, T. Wang, J. Feng, D. Yang, S. Perrett, and X. Yan, Nat. Nanotechnol. **2**(9), 577–583 (2007).